

Preparation of hybrid Josephson junctions on Co-doped Ba-122 single crystals

D Reifert^{1‡}, N Hasan¹, S Döring¹, S Schmidt¹, M Monecke^{1§},
M Feltz¹, F Schmidl¹, V Tympel¹, W Wisniewski², I Mönch³,
T Wolf⁴, P Seidel¹

¹Institute of Solid State Physics, Friedrich-Schiller-University Jena, Helmholtzweg 5, 07743 Jena, Germany

²Otto-Schott-Institut of Materials Research, Friedrich-Schiller-University Jena, Fraunhoferstrasse. 6, 07743 Jena, Germany

³Institute for Integrative Nanosciences, IFW Dresden, Helmholtzstrasse 20, 01171 Dresden, Germany

⁴Institute of Solid State Physics, Karlsruhe Institute of Technology, 76021 Karlsruhe, Germany

E-mail: sebastian.doering.1@uni-jena.de

Abstract. In this paper we present a method for processing a hybrid Josephson junction on Co-doped BaFe₂As₂ (Ba-122) single crystals with a thin film Pb-counter electrode and a barrier layer of TiO_x. This includes the leveling and polishing of the crystals and structuring them with thin film techniques such as photo lithography, sputtering and ion beam etching (IBE). The junctions show hysteretical resistively and capacitively shunted junction (RCSJ)-like I - V characteristics with an $I_c R_n$ -product of about 800 μ V.

‡ Present address: Physikalisch-Technische Bundesanstalt (PTB), Bundesallee 100, D-38116 Braunschweig, Germany

§ Present address: Chemnitz University of Technology, Physics Department / Semiconductor Physics, Reichenhainer Strasse 70, 09126 Chemnitz, Germany

1. Introduction

Single crystals are an ideal tool to investigate the basic properties of a new material due to their nearly perfect crystalline structure. On the other hand Josephson junctions are a good method to investigate the electrical properties of a superconductor. Despite this, only little literature about Josephson junctions on pnictide single crystals[1, 2, 3] could be found by the authors. This could be due to the surface properties of pnictide single crystals, e.g. roughness and degradation in a normal atmosphere[4], and the lack of in-situ preparability of artificial barriers. In the literature mentioned above the single crystals used as one electrode were coupled by point contacts, thick films or even crossed by other single crystals, making the junction area and barrier type difficult to control. Our approach enables us to produce controllable junctions with areas ranging from $5 \times 5 \mu\text{m}^2$ to $50 \times 50 \mu\text{m}^2$ using normal conducting and insulating barriers, which is advantageous for future systematic investigations of the junction properties. We typically used a junction area of $15 \times 15 \mu\text{m}^2$ for the investigation of TiO_x as an insulating material. Polishing the crystal surface is necessary in order to prepare these junctions using photolithography, sputtering and IBE. Therefore we developed a polishing procedure for these crystals which, to the best of our knowledge, has not been done before.

2. Sample Preparation

The $\text{Ba}(\text{Fe}_{1-x}\text{Co}_x)_2\text{As}_2$ crystals we used were grown from self-flux in glassy carbon crucibles in analogy to references [5,

6]. A particularly low cooling rate of 0.3°C/h was applied to minimize the amount of flux inclusions and crystal defects. The composition of the crystals was determined by energy dispersive X-ray spectroscopy to be $\text{Ba}(\text{Fe}_{1-x}\text{Co}_x)_2\text{As}_2$ with $x = 0.054$. A critical temperature T_c of 23.5 K was inductively measured. Figure 1 shows an optical micrograph of a typical unprocessed single crystal. The surface shows significant structures covering the main plateau. The measurements with atomic force microscopy (AFM) presented in figure 2 show, that these are steps with a height of several nm to several μm . The crystal orientation of

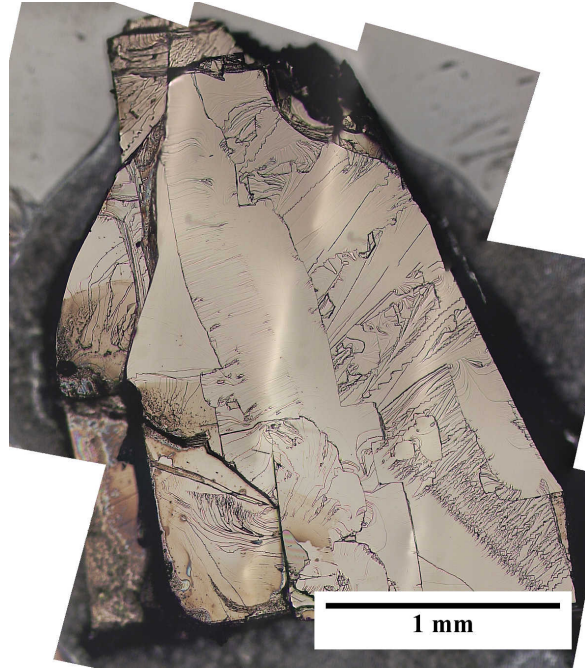


Figure 1. Microscope image of a Ba-122 single crystal as-grown.

some undoped crystals was analysed using electron backscatter diffraction (EBSD) in a Jeol JSM-7001F equipped with an EDAX Trident analysing system containing a TSL Digiview 1913 EBSD-camera. EBSD-scans were captured and evaluated using the

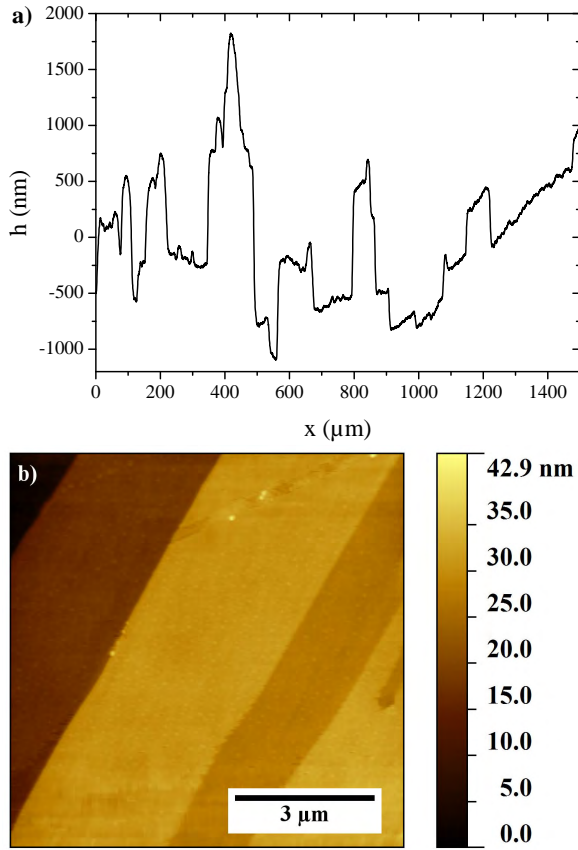


Figure 2. a) Topographical profile of the unprocessed surface with a step height of up to several μm . b) AFM measurement of the same surface featuring additional nanoscopic steps.

programs TSL OIM Data Collection 5.31 and TSL OIM Analysis 5. The scans were performed using a current of about 2.40 nA (measured with a Faraday cup) and a voltage of 20 kV. Figure 3 presents an scanning electron microscopy (SEM) image of the central plateau of one sample tilted by 20° to enhance the topographical contrast. The EBSD-pattern presented in the figure is representative for the BaFe_2As_2 patterns obtained from the entire extent of the sample with only minimal deviations. A material file for indexing the patterns was built using the data of

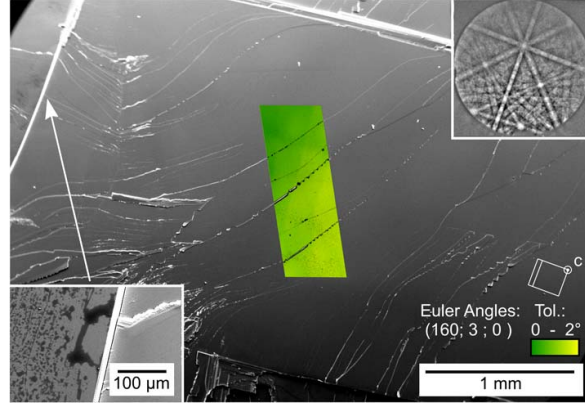


Figure 3. SEM-micrograph of a crystal surface superimposed by the orientation+IQ map of a performed EBSD-scan. The presented EBSD-pattern is representative for patterns obtained from the extremities and centre of the sample. The inset features the edge of the main plateau to adjacent areas where a second phase (dark) is frequently observed.

ICSD-File no. 169555. The combined orientation+image quality (IQ) map of an EBSD-scan performed on the surface is superimposed on the SEM-micrograph. It shows that the crystal orientations deviate less than 2° from the defined Euler Angle triplet (160;3;0) illustrated by the wire frame of the unit cell (right). The crystallographic c-axis of this tetragonal crystal is hence tilted by about 3° from the normal of the SEM-stage. The inset to the left shows the edge of the plateau in greater detail where a second phase enriched in carbon is frequently observed. EBSD-patterns could not be obtained from this phase indicating it may be amorphous. The inclusions of this phase were not observed on the main plateau of the crystal and are hence neglected during further analysis.

The surface needed to be polished,

because of the thin film technologies used to apply barrier thicknesses down to 2 nm. The crystals were embedded in an epoxy resin and mounted on an oxidised silicon wafer to enhance handling during the three step polishing process. The surface was initially planarised by lapping in the Logitech PM5 Lapping & Polishing System using alumina powder of $3\mu\text{m}$ grain size suspended in water-free isopropyl alcohol due to the sensitivity of the crystal to corrosion by water. The resulting surface showed a roughness of about $1\mu\text{m}$ root mean square (RMS). Subsequently, the samples were polished using decreasing grain sizes of SiC polishing foil to reduce the roughness to ca. 10 nm RMS. The final step again performed on the PM5 system using alumina powder of 50 nm grain size suspended in isopropyl alcohol. A relatively high load of 1.8 kg enabled to achieve a roughness of 0.6 nm to 2.0 nm RMS, see figure 4.

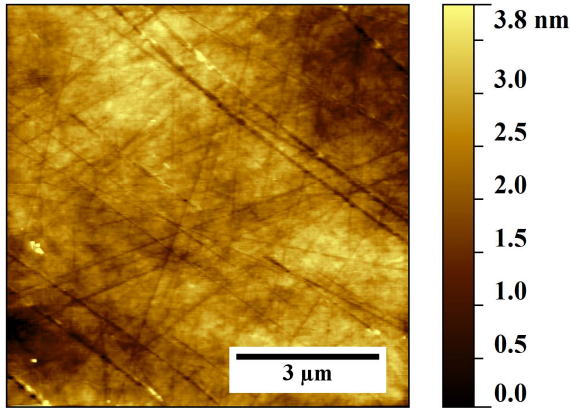


Figure 4. AFM measurement of a polished crystal surface with a RMS roughness of 0.6 nm.

An Au protection layer of 50 nm was deposited on the samples via DC sputtering directly after polishing, similar to the process used for thin film junctions [8]. This

avoids future degradation of the freshly polished surface during further preparation. The applied junction design allows the electrical characterisation of the junction and of both electrodes in 4-probe geometry and is outlined in figure 5. The

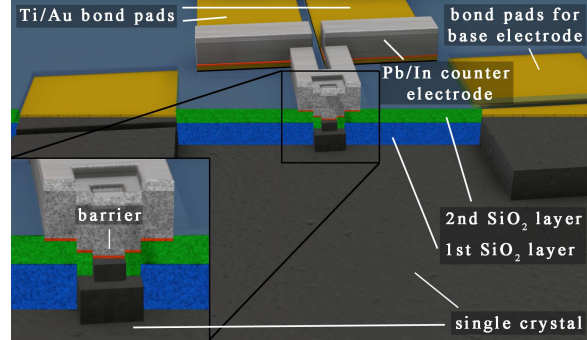


Figure 5. Scheme of the junction design. The inset shows the junction interface in greater detail.

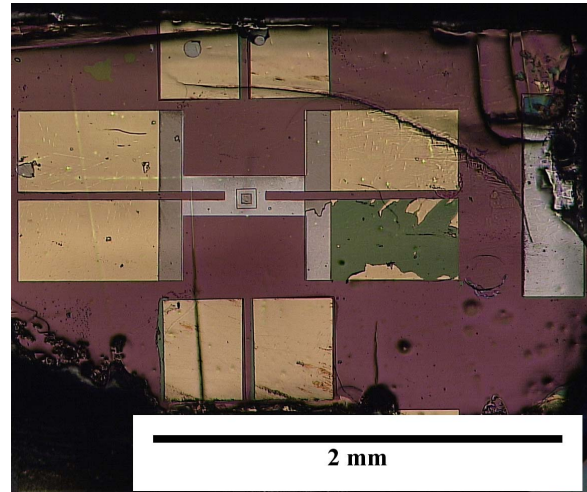


Figure 6. Optical micrograph of a final junction. The distorted bond pad on the right was probably caused by surface contamination. This lead to a decreased adherence of the Ti/Au system.

Ba-122 crystal acts as the base electrode, which is fully insulated from the Pb counter electrode by two layers of SiO_2 . The Ti/Au

bond pads necessary for the electrical contacting through thermosonic wirebonding are also illustrated.

This junction setup was achieved by first etching 100 nm into the crystal, using an Ar ion beam (beam voltage = 500 V, fluence = 0.9 mA/cm²) and a photo lithography mask. The Au protection layer is simultaneously removed from these regions and hence can not act as a parasitic parallel shunt on the crystal surface. A 200 nm thick SiO₂ layer was subsequently deposited via reactive high frequency (HF) sputtering using a deposition rate of 2.5 nm/min. This first insulating layer opens a big primary window for the future junction area. After a lift-off the next photo lithography mask was applied. The sample was again patterned through IBE, followed by the deposition of a second 200 nm thick SiO₂ layer with a smaller window, which defines the actual junction area. After another lift-off, the mask for the bonding pads of the counter electrode was applied. Now a third SiO₂ layer of 100 nm was deposited to improve the insulation between the base electrode and the bonding pads of the counter electrode. An additional Ti/Au bi-layer was deposited by DC sputtering to increase the adhesive strength of the bonding pads. The Ti layer was deposited with a deposition rate of about 0.4 nm/s while the Au layer was deposited in-situ with a deposition rate of about 1 nm/s. The junction interface was cleaned by IBE after the lift-off and fabrication of the counter electrode mask. The existing gold layer is removed during the cleaning step and the etching time was calculated to stop at the gold/pnictide interface in order to avoid the degradation of Ba-122. A thin Ti layer of 1.5 to

10 nm was subsequently deposited by DC sputtering and oxidised in a normal atmosphere at a temperature of 80 °C to form a TiO_x barrier. Finally, thermal evaporation was used to deposit the 300 nm thick Pb counter electrode ex-situ (deposition rate = 0.5 nm/s) and an In cap layer (50 nm) in-situ to protect the Pb layer from degradation. After a final lift-off, the complete junction as shown in figure 6 is ready for electrical measurements.

3. Electrical measurements

The measurements were realised in a helium dewar in which the sample was cooled to the temperature of liquid helium. A typical I - V characteristic of a Josephson junction measured at $T = 4.2$ K is presented in figure 7.

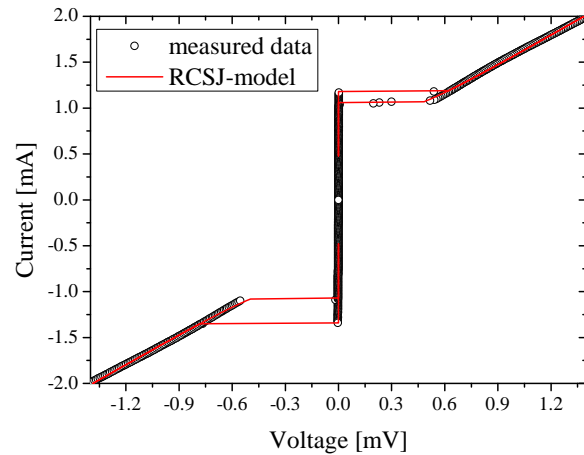


Figure 7. Measured I - V characteristic of a Josephson junction at $T = 4.2$ K compared to a fit within the RCSJ-model. The used fitting parameters are mentioned in the text. The junction area was $15 \times 15 \mu\text{m}^2$, while the thickness of the titanium oxide barrier was about 10 nm.

In figure 7 we compared our measurement to the prediction of the RCSJ model

[9, 10]. In order to match our data we expanded the model by an excess current. Additionally the fit was executed separately for positive and negative currents, because the measurement shows a significant asymmetry. The fit yields an I_c of $770\mu\text{A}$ for positive currents and $947\mu\text{A}$ for negative currents, with a symmetric excess current of $400\mu\text{A}$ and normal state resistance R_n of 0.87Ω . The McCumber parameters are 1.76 (positive) and 3.11 (negative), respectively. This leads to $I_c R_n$ -products of $668\mu\text{V}$ (positive) and $829\mu\text{V}$ (negative). Former publications on Josephson junctions with a conventional superconductor electrode [1, 2, 11, 12], but also all-pnictide junctions [3, 13, 14, 15], did not show such a high $I_c R_n$ -product.

4. Summary

We described a polishing process that enables us to achieve a high quality surface on Ba-122 single crystals. On this surface we can prepare Josephson junctions using the classical thin film technologies photo lithography, IBE and sputtering. The junction layout we used was derived from earlier thin film junctions and will be optimised for single crystals in the future. Furthermore we presented some electrical measurements of the Josephson effect on these junctions, where a high $I_c R_n$ -product could be observed.

5. Acknowledgements

This work was funded within the European Community project IRON-SEA under grant number FP7-283141 and by the German Research Community (DFG) within priority program 1458 under grant

number SE664/15-2. S. Schmidt was funded by the Landesgraduiertenförderung Thüringen and N. Hasan was funded by the German Academic Exchange Service (DAAD).

References

- [1] Zhang X, Oh Y S, Liu Y, Yan L, Kim K H, Greene R L and Takeuchi I 2009 *Phys. Rev. Lett.* **102** 147002
- [2] Zhou Y R, Li Y R, Zuo J W, Liu R Y, Su S K, Chen G F, Lu J L, Wang N L and Wang Y P 2008 *arXiv* **0812.3295** (*Preprint* 0812.3295)
- [3] Zhang X, Saha S R, Butch N P, Kirshenbaum K, Paglione J, Greene R L, Liu Y, Yan L, Oh Y S, Kim K H and Takeuchi I 2009 *Appl. Phys. Lett.* **95** 062510
- [4] Plecenik T, Gregor M, Sobota R, Truchly M, Satrapinsky L, Kurth F, Holzapfel B, Iida K, Kus P and Plecenik A 2013 *Appl. Phys. Lett.* **103** 052601
- [5] Hardy F, Adelman P, Wolf T, v Löhneysen H and Meingast C 2009 *Phys. Rev. Lett.* **102** 187004
- [6] Hardy F, Wolf T, Fisher R A, Eder R, Schweiss P, Adelman P, v Löhneysen H and Meingast C 2010 *Phys. Rev. B* **81** 060501
- [7] URL <http://gwyddion.net/>
- [8] Döring S, Schmidt S, Schmidl F, Tympel V, Haindl S, Kurth F, Iida K, Mönch I, Holzapfel B and Seidel P 2012 *Physica C: Superconductivity* **478** 1518
- [9] McCumber D E 1968 *J. Appl. Phys.* **39** 3113–3118
- [10] Stewart W C 1968 *Appl. Phys. Lett.* **12** 277–280
- [11] Schmidt S, Döring S, Schmidl F, Grosse V, Seidel P, Iida K, Kurth F, Haindl S, Mönch I and Holzapfel B 2010 *Appl. Phys. Lett.* **97** 172504
- [12] Döring S, Schmidt S, Schmidl F, Tympel V, Haindl S, Kurth F, Iida K, Mönch I, Holzapfel B and Seidel P 2012 *Supercond. Sci. Technol.* **25** 084020
- [13] Katase T, Ishimaru Y, Tsukamoto A, Hiramatsu H, Kamiya T, Tanabe K and Hosono H 2010 *Appl. Phys. Lett.* **96** 142507

- [14] Katase T, Isimaru Y, Tsukamoto A, Hiramatsu H, Kamiya T, Tanabe K and H H 2011 *Nature Comm.* **2** 409
- [15] Schmidt S, Doring S, Schmidl F, Tympel V, Haindl S, Iida K, Kurth F, Holzapfel B and Seidel P 2013 *IEEE Trans. Appl. Supercond.* **23** 7300104 ISSN 1051-8223